STANDARD MICROSOURCE INTERFACE FOR A MICROGRID

Prabath Janaka BINDUHEWA
University of Manchester, UK
prabath@theiet.org

Mike BARNES
University of Manchester, UK
mike.barnes@manchester.ac.uk

Alasdair RENFREW
University of Manchester, UK
alasdiar.renfrew@manchester.ac.uk

ABSTRACT

The plug-and-play functionality of a typical MicroGrid should enable the connection of any microsource at any point without changing the system significantly. To achieve this feature, this paper presents a 'standard' microsource interface concept with embedded with storage in the form of ultracapacitors. The photovoltaic panel, which is the microsource, is connected to the MicroGrid through an inverter and the storage is connected to the dc-link via a bi-directional converter. Simulation results of the complete interface are presented.

INTRODUCTION

A collection of microsources providing electricity and heat to local users, and which is capable of both autonomous and grid-connected operation, is known as a MicroGrid which is shown in Figure 1 [1, 2]. Such a system could potentially reduce transmission and distribution losses significantly and might be used to defer utility system reinforcement.

The microsources which might be connected in a MicroGrid include photovoltaics, small wind turbines, biogas and hydro power. Particularly important is the use of combined heat and power plants, which increase the overall calorific efficiency of the MicroGrid system. Such microsources have little or no rotational inertia [2] compared with conventional generating plant. Thus for stable operation of the system, some form of energy storage is essential. While the storage could be either centralised or distributed, the plug-and-play functionality requirement of a MicroGrid, means distributed storage is more suitable.

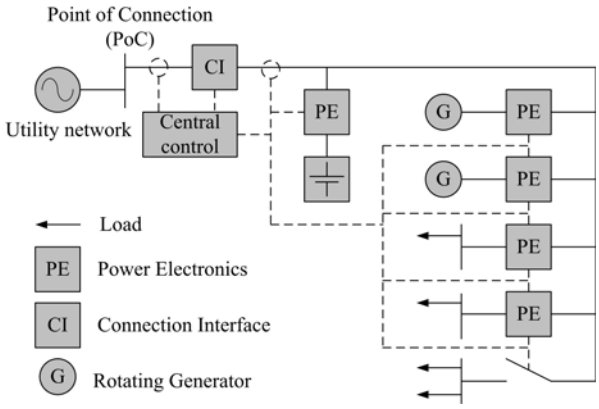

Figure 1: Example MicroGrid

Integrating the distributed storage into the microsource unit also allows the dynamics of the microsource to be decoupled from the system, potentially allows the microsource power electronics to be partly utilised, and also may facilitate limited time-shifting of micro-generated energy. This paper presents such microsource interface concept. Similar concepts have been presented for large CHP units employing battery energy storage [3]. The study is carried out in EMTDC/PSCAD™ software.

PROPOSED SYSTEM

The proposed microsource interface with embedded storage is shown in Figure 2. The microsource, storage and power electronic converters are the main components of the proposed interface. The microsource, in this case photovoltaic panel, is connected to the inverter through a dc-dc converter. The dc-dc converter ensures that the panel operates at its Maximum Power Point (MPP). It also steps up the panel voltage.

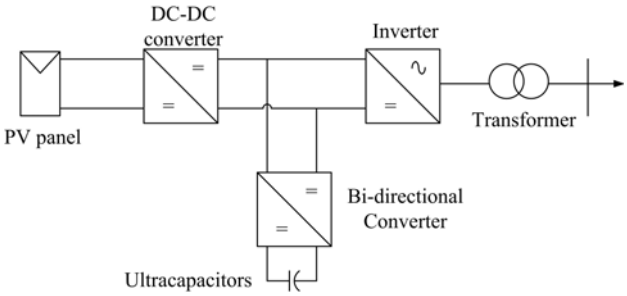

Figure2: Proposed microsource interface

The dc voltage at the dc-link is converted to three-phase ac by mean of a three-phase voltage source inverter. The frequency and the voltage of the inverter are controlled using the terminal quantities. The transformer acts as the coupling inductor. Further, it steps up the voltage and removes any residual dc current injection. It should be appreciated that while the example shown here is three-phase, the inverter interface in many microsources may be single-phase.

Due to variation in the ambient conditions, the output power of the PV panel will vary with time. This would introduce variations in the dc-link. The dynamics of the dc-link could make the controller of the inverter complicated. In the proposed system dc-link voltage is kept approximately constant by interfacing storage to the dc-link via a bi-directional converter.

PHOTOVOLTAIC PANEL MODELLING

In order to analyse the system dynamics, it is necessary to model the photovoltaic panel. The data of the HIP-205BE11 panel was used for modelling purposes. The relationship between output voltage and current of a PV panel is given by the characteristic equation (1). The panel was modelled

using a controllable voltage source. The block diagram of the PV model is presented in the Figure 3 where the irradiance and the temperature are the inputs. In order to avoid numerical instabilities, an inductor is inserted series to the voltage source. It is possible to represent the voltage at maximum power point as a fraction of the open circuit voltage. This property is used to extract the voltage at the MPP in the analysis. Figure 4 shows the characteristic curve obtained from the simulation model.

$$I_{PV} = I_{ph} - I_{sat}\left[\exp\left(\frac{V_{pv} + I_{pv}R_s}{V_t}\right) - 1\right] \quad (1)$$

Where I_{pv}, I_{ph}, I_{sat}, V_{pv}, R_s and V_t are PV panel output current, photocurrent, saturation current, PV panel voltage, series resistance and thermal voltage.

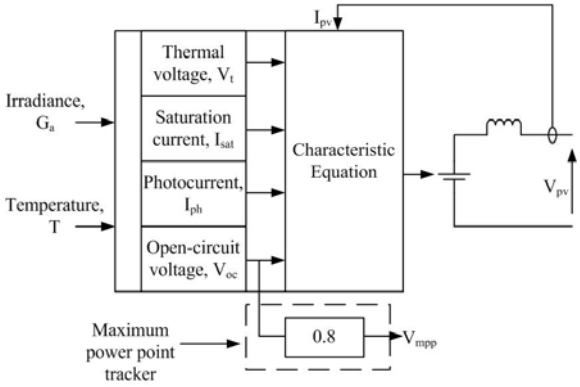

Figure 3: Block diagram of the PV panel model [4, 5]

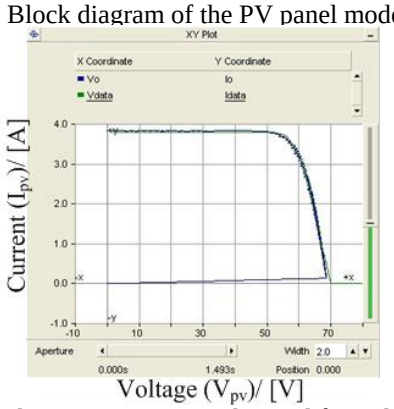

Figure 4: Characteristic curve obtained from the model

DC-DC CONVERTER INTERFACE

The dc-dc converter steps up the photovoltaic panel voltage and ensures that the PV panel is operating at the maximum power point. As shown in Figure 5, the inner control loop of the converter ensures that the input voltage to the converter is kept constant. PV panel operating at MPP would be ensured by the outer control loop [5]. According to the PV model, MPP voltage depends on the temperature. Figure 6 shows the variation of the voltage of panel at MPP during temperature changes. The controller of the dc-dc converter should respond to this MPP change and results shown in Figure 6 illustrate the change of the PV panel voltage according the MPP voltage change.

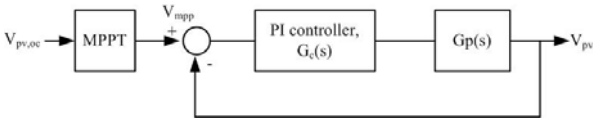

Figure 5: Controller of the dc-dc converter

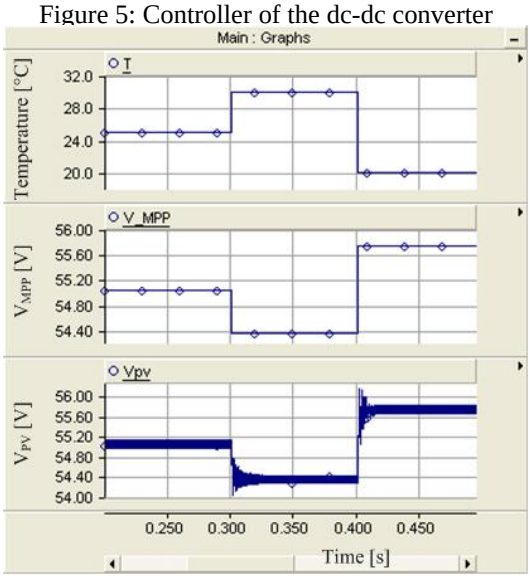

Figure 6: PV panel connected with dc-dc converter

STORAGE AND BI-DIRECTIONAL CONVERTER

There are several possible storage methods: batteries, ultracapacitors and flywheels. The function of the storage in this application is to smooth out the transients. As a result the storage should have high power density but should be low maintenance. Therefore ultracapacitors were selected as the storage method.

The ultracapacitor storage is interconnected to the dc-link through the bi-directional converter. The function of the controller of the bi-directional converter is to keep the dc-link voltage approximately constant. As shown in Figure 7, the bi-directional converter operates in step down mode if the dc-link voltage is above the higher reference value and operates in step down mode when the dc-link voltage is below the lower reference. During step down mode, energy is transferred into the storage unit while energy is fed into the dc-link during step up mode. With this control technique, large variations in the dc-link due output variation in PV panel could be prevented.

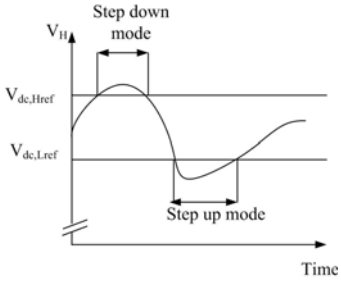

Figure 7: Control method of the bi-directional converter [5]

THREE-PHASE INVERTER AND TRANSFORMER

A three-phase voltage source inverter would convert the dc voltage into three-phase ac voltage. The three-phase transformer connected to the inverter acts as the coupling inductor. A dq control technique is used to control the inverter. The inverter is to be controlled using the terminal quantities of the point of common coupling. Figure 8 shows the inverter with coupling inductor and the resistor. Equation (2) presents the relationship between inverter output voltage, point of coupling voltage and the current.

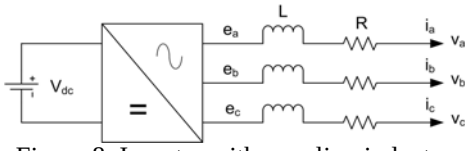

Figure 8: Inverter with coupling inductor

$$\begin{bmatrix} e_a - v_a \\ e_b - v_b \\ e_c - v_c \end{bmatrix} = \left(R + L\frac{d}{dt} \right) \begin{bmatrix} i_a \\ i_b \\ i_c \end{bmatrix} \quad (2)$$

By taking the abc-dq conversion and Laplace transform respectively, the following well-known equations can be obtained.

$$i_d = \frac{1}{Ls}\left[e_d - v_d - Ri_d - \omega L i_q \right] \quad (3)$$

$$i_q = \frac{1}{Ls}\left[e_q - v_q - Ri_q + \omega L i_d \right] \quad (4)$$

Figure 9(a) presents the system and the controller block diagram. Equation (3) and (4) are represented in the system. In the controller, cross-coupling terms are removed from the measurement signals. Thereby the system could be reduced to first order. The simplified new system is shown in Figure 9(b). In a practical system, set values could be used for disturbance decoupling, if noise in measured values is a problem.

According to [3], the transformer and the inductor should be sized to ensure that the voltage angle across the inductance is 10° at the full power. Further according to [6], a typical X/R ratio for a distribution system is around 10, which is used for this analysis.

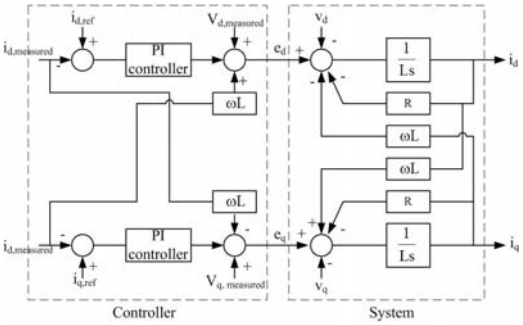

(a) Controller and the system

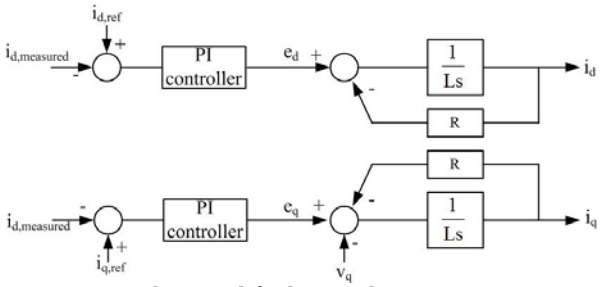

(b) Simplified control system

Figure 9: Controller and the system block diagram after removing the cross coupled terms

For the purpose of this study the d-axis current reference is derived from the PV panel output power as shown in Figure 10. The PV panel output power is calculated from the PV panel voltage and current measurements. With the aid of approximated efficiencies of the dc-dc converter and inverter, output power of the inverter is calculated. Thereby the d-axis reference current is calculated. The q-axis current reference is set to zero. In practice some form of feedback will be required to compensate for the difference between expected converter efficiency and actual converter efficiency.

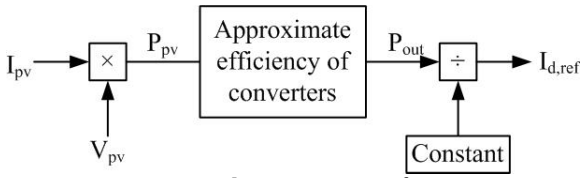

Figure 10: d-axis current reference

RESULTS

The system contains three controllers which control the dc-dc converter, bi-directional converter and the inverter. The developed microsource interface was connected to a distribution system shown in Figure 11. The system response to the irradiance change is examined.

According to Figure 12, as irradiance increases the output power of the PV panel increases. Therefore an increase in output current from the inverter occurs. As a result, the current delivered from the distribution system reduces. According to Figure 13, a reduction of PV output power occurs during an irradiance reduction. As a result the inverter output current is reduced. Current delivered by the distribution system is increased to power the load. In both cases, the dc-link voltage is approximately kept constant. Thus the dc-link dynamics are reduced by the storage which is connected to the dc-link via a bi-directional converter.

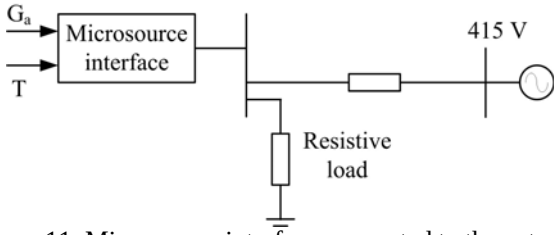

Figure 11: Microsource interface connected to the network

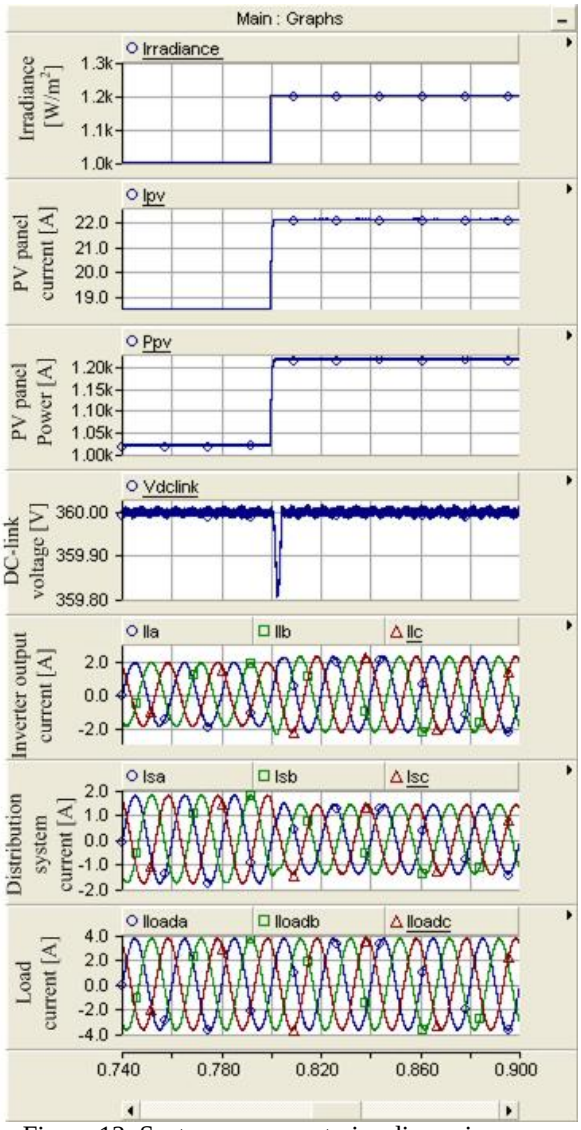

Figure 12: System response to irradiance increase

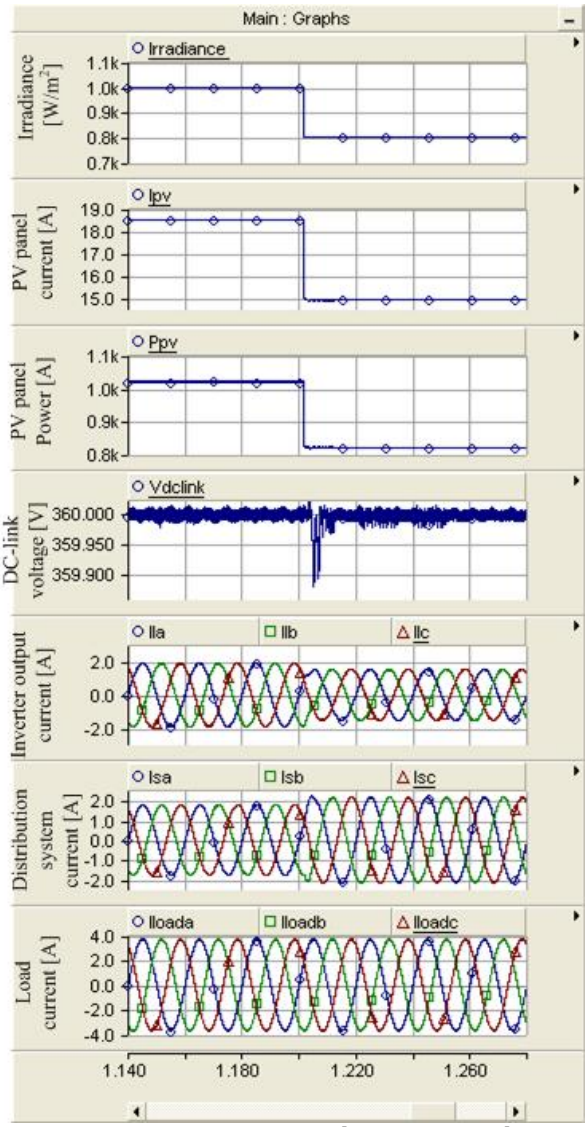

Figure 13: System response to decrease in irradiance.

CONCLUSION

A microsource interface concept with an ultracapacitor storage unit is shown. The system was connected to a distribution network with rated load. The system response to the irradiance variation, which varies the PV panel output power, is simulated. According to the results the system is behaving as expected.

ACKNOWLEDGEMENT

Authors appreciate for the support received by the EPSRC grant EP/C00177X/1 'UK-MicroGrids' to conduct this research.

REFERENCES

[1] B. Lasseter, 2001, "Microgrids", *IEEE Power Engineering Winter Meeting*, vol. 1, 146-149

[2] R.H. Lasseter, 2002, "MicroGrids", *IEEE Power Engineering Society Winter Meeting*, vol. 1, 305-308

[3] P. Piagi, R.H. Lasseter, 2006, "Autonomous control of Microgrids", *IEEE Power Engineering Society General Meeting*, 8pps

[4] P.J. Binduhewa, A.C. Renfrew, M. Barnes, 2008, "MicroGrid Power Electronics Interface for Photovoltaics", *the 4th International Conference on Power Electronics, Machines and Drives*, 260-264

[5] P.J. Binduhewa, A.C. Renfrew, M. Barnes, 2008, "Ultracapacitor Energy Storage for MicroGrid Micro-generation", *the 4th International Conference on Power Electronics, Machines and Drives*, 270-274

[6] B.M. Weedy, 1992, *Electric Power Systems*, John Wiley & Sons, Great Britain, 270.